

Synthesis, Characterization, and Calculated Electronic Structure of the Crystalline Metal–Organic Polymers $[\text{Hg}(\text{SC}_6\text{H}_4\text{S})(\text{en})]_n$ and $[\text{Pb}(\text{SC}_6\text{H}_4\text{S})(\text{dien})]_n$

Dayna L. Turner,^{†,⊥} Kevin H. Stone,^{‡,||} Peter W. Stephens,[‡] Aron Walsh,[§] Mayank Pratap Singh,[†] and Thomas P. Vaid*[†]

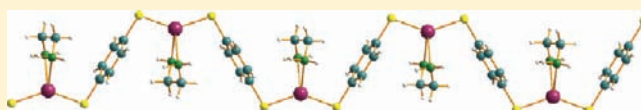
[†]Department of Chemistry, The University of Alabama, Tuscaloosa, Alabama 35487, United States

[‡]Department of Physics and Astronomy, Stony Brook University, Stony Brook, New York 11794, United States

[§]Centre for Sustainable Chemical Technologies and Department of Chemistry, University of Bath, Claverton Down, Bath BA2 7AY, U.K.

Supporting Information

ABSTRACT: The reaction of $\text{Hg}(\text{OAc})_2$ with 1,4-benzenedithiol in ethylenediamine at 80 °C yields $[\text{Hg}(\text{SC}_6\text{H}_4\text{S})(\text{en})]_n$, while the reaction of $\text{Pb}(\text{OAc})_2$ with 1,4-benzenedithiol in diethylenetriamine at 130 °C yields $[\text{Pb}(\text{SC}_6\text{H}_4\text{S})(\text{dien})]_n$. Both products are crystalline materials, and structure



determination by synchrotron X-ray powder diffraction revealed that both are essentially one-dimensional metal–organic polymers with $-\text{M}-\text{SC}_6\text{H}_4\text{S}-$ repeat units. Diffuse reflectance UV–visible spectroscopy indicates band gaps of 2.89 eV for $[\text{Hg}(\text{SC}_6\text{H}_4\text{S})(\text{en})]_n$ and 2.54 eV for $[\text{Pb}(\text{SC}_6\text{H}_4\text{S})(\text{dien})]_n$, while density functional theory (DFT) band structure calculations yielded band gaps of 2.24 and 2.10 eV, respectively. The two compounds are both infinite polymers of metal atoms linked by 1,4-benzenedithiolate, the prototypical molecule for single-molecule conductivity studies, yet neither compound has significant electrical conductivity as a pressed pellet. In the case of $[\text{Pb}(\text{SC}_6\text{H}_4\text{S})(\text{dien})]_n$ calculations indicate fairly flat bands and therefore low carrier mobilities, while the conduction band of $[\text{Hg}(\text{SC}_6\text{H}_4\text{S})(\text{en})]_n$ does have moderate dispersion and a calculated electron effective mass of $0.29 \cdot m_e$. Hybridization of the empty Hg 6s orbital with $\text{SC}_6\text{H}_4\text{S}$ orbitals in the conduction band leads to the band dispersion, and suggests that similar hybrid materials with smaller band gaps will be good semiconductors.

INTRODUCTION

Hybrid organic–inorganic materials have been receiving increasing attention because they offer structures and properties not attainable in purely organic or inorganic materials. The most prominent class of hybrid materials is metal–organic frameworks (MOFs),^{1–5} which often have very high porosities and are being examined as materials for gas storage,⁶ separation,⁷ and sensing.⁸ The vast majority of well-defined hybrid organic–inorganic materials (including MOFs) are electrical insulators and are diamagnetic or paramagnetic at room temperature, and hybrid materials with interesting electrical or magnetic properties are therefore ripe for further investigation.⁹ In known hybrid materials there is generally poor electronic communication between metal centers across the organic bridges, and one reason may be the large electronegativity difference in the metal–oxygen and metal–nitrogen linkages that form those networks. We have been studying hybrid materials that contain instead metal–sulfur and metal–selenium linkages in an effort to find semiconducting materials.^{10,11}

The compounds reported in this paper, $[\text{Hg}(\text{SC}_6\text{H}_4\text{S})(\text{en})]_n$ and $[\text{Pb}(\text{SC}_6\text{H}_4\text{S})(\text{dien})]_n$ ($\text{SC}_6\text{H}_4\text{S}$ is 1,4-benzenedithiolate, en is ethylenediamine, and dien is diethylenetriamine), are one-dimensional polymers, and therefore represent particularly simple examples of the metal–chalcogen–organic hybrid materials that we have been investigating. The organic and

inorganic components of these polymers have been studied separately as electrically conducting molecules: the 1,4-benzenedithiolate linker is probably the most-studied entity in single-molecule conductivity investigations,^{12–15} and, more recently, the single-molecule conductivity of small metal–chalcogenide clusters has been reported.¹⁶ The polymers $[\text{Hg}(\text{SC}_6\text{H}_4\text{S})(\text{en})]_n$ and $[\text{Pb}(\text{SC}_6\text{H}_4\text{S})(\text{dien})]_n$ can be viewed as infinite arrays of metal atoms linked by 1,4-benzenedithiolate, or, alternatively, as the smallest possible HgS or PbS units linked by phenylene bridges. The physical characterization and band-structure calculation of these simple polymers give insight into their electronic structure and suggest modifications to achieve better electrical conductivity in new metal–chalcogenide–organic network materials.

EXPERIMENTAL SECTION

General Synthetic Procedures and Materials. Reactions were carried out under N_2 in degassed ethylenediamine or degassed diethylenetriamine; the products are air-stable for periods of at least a few hours, and the workup and subsequent handling was done without protection from air, although the products were then stored in a nitrogen-filled glovebox. Reagents were purchased from commercial

Received: August 17, 2011

Published: December 2, 2011

suppliers and used as received. The reagent 1,4-benzenedithiol was prepared from 1,4-bis(isopropylthio)benzene,¹⁷ which was reduced by sodium in liquid ammonia to yield 1,4-benzenedithiol.¹⁸

[Hg(SC₆H₄S)(en)]_n. Mercury acetate (224 mg, 0.703 mmol) and 1,4-benzenedithiol (100 mg, 0.703 mmol) were combined in 10 mL of ethylenediamine. The suspension was heated to 80 °C for 16 h and then cooled to room temperature. The pale yellow precipitate was isolated by filtration and washed with methanol and ether. Yield of [Hg(SC₆H₄S)(en)]_n: 218 mg, 77%. IR (Nujol, cm⁻¹): 3324 (m), 3272 (m), 1582 (s), 1125 (w), 1096 (s), 1084 (w), 1012 (s), 974 (s), 946 (s), 824 (s), 666 (w). Anal. Calc. for C₈H₁₂N₂S₂Hg: C, 23.97; H, 3.02; N, 6.99. Found: C, 23.16; H, 1.79; N, 5.39.

[Pb(SC₆H₄S)(dien)]_n. Lead(II) acetate trihydrate (133 mg, 0.351 mmol) and 1,4-benzenedithiol (50 mg, 0.352 mmol) were combined in 12 mL of diethylenetriamine. The suspension was heated to 130 °C for 16 h and then cooled to room temperature. The bright yellow solid was isolated by filtration and washed with methanol and then diethylether. Yield of [Pb(SC₆H₄S)(dien)]_n: 144 mg, 91%. IR (Nujol, cm⁻¹): 3356 (w), 3326 (w), 3192 (m), 3107 (w), 1570 (w), 1316 (w), 1227 (w), 1139 (w), 1095 (s), 1006 (w), 990 (w), 899 (s), 867 (w), 818 (m), 668 (w). Anal. Calc. for C₁₀H₁₇N₃S₂Pb: C, 26.66; H, 3.80; N, 9.33. Found: C, 26.63; H, 3.77; N, 9.01.

Room-temperature solid-state conductivity of pressed powders was measured as described previously,¹⁹ in a two-electrode configuration on a lab-built apparatus that consists of a Delrin block with a 6.35 mm diameter cylindrical hole and two 6.35 mm copper cylindrical contacts. The material to be studied was inserted between the two contacts within the Delrin block and a mass of 3.85 kg was placed on the top contact, thus applying 12 bar pressure.

Diffuse reflectance UV–visible–NIR spectra were obtained on a Shimadzu UV-3600 spectrometer with a Harrick Praying Mantis accessory. A Spectralon disk was used as the reflectance standard. Percent reflectance was converted to absorbance by the formula $\text{abs} = \log_{10}(100/\%R)$.

Synchrotron X-ray Diffraction. The crystal structures of both materials were solved from high resolution synchrotron X-ray powder diffraction data collected at beamline X16C at the National Synchrotron Light Source at Brookhaven National Laboratory at ambient temperature. Both materials were loaded into thin walled glass capillaries, illuminated with X-rays of ~0.7 Å wavelength, and spun during data collection for improved powder averaging. The diffracted beam was analyzed with a Ge(111) crystal and detected by a NaI scintillation counter. Structures were indexed, solved by simulated annealing, and Rietveld refined using the TOPAS-Academic software.²⁰

Computational Techniques. Electronic structure calculations were performed for [Hg(SC₆H₄S)(en)]_n and [Pb(SC₆H₄S)(dien)]_n at the level of density functional theory (DFT)^{21,22} within the generalized gradient approximation (the PBEsol exchange-correlation functional)²³ as implemented in the all-electron code FHI-AIMS.^{24,25} Periodic boundary conditions in three dimensions were employed to represent the infinite solid.²⁶ A well converged “tight” numerical basis set was used to construct the electronic wave function, with scalar relativistic effects treated at the scaled-ZORA level of theory.²⁷ Comparison of the calculated electronic structure of a Hg(II) compound, HgO, arising from this approach with results from a previous DFT study using a plane-wave basis set²⁸ showed excellent agreement, and reproduced the measured X-ray photoemission spectra.²⁹ The equilibrium (*T* = 0 K) structural parameters for both [Hg(SC₆H₄S)(en)]_n and [Pb(SC₆H₄S)(dien)]_n were determined through minimization of the quantum mechanical forces and stresses to within 0.005 eV/Å.

RESULTS AND DISCUSSION

Synthesis. The compounds [Hg(SC₆H₄S)]_n and [Pb(SC₆H₄S)]_n (without any donor ligands) were reported in 1975.³⁰ [Hg(SC₆H₄S)]_n (yellow) was synthesized in 2,4-lutidine, and [Pb(SC₆H₄S)]_n (brown) was synthesized in a water–methanol mixture. [Hg(SC₆H₄S)]_n did display a small amount of

electrical conductivity at 60 °C. However, both compounds were completely amorphous and could not be structurally characterized. The use of ethylenediamine or diethylenetriamine as a solvent, as described below, leads to crystalline products.

The synthesis of [Hg(SC₆H₄S)(en)]_n is similar to that of [Pb₃(SC₆H₄S)₃(en)₂]_n,¹⁰ [Cd(en)₃][Cd(SC₆H₄S)₂]_n,¹¹ and [Zn(en)₃][Zn(SC₆H₄S)₂]_n¹¹ reported previously. The reaction of Hg(OAc)₂ with 1,4-benzenedithiol in ethylenediamine at 80 °C yields a pale yellow precipitate of [Hg(SC₆H₄S)(en)]_n. The synthesis of [Pb(SC₆H₄S)(dien)]_n is quite similar to that of [Pb₃(SC₆H₄S)₃(en)₂]_n with the substitution of diethylenetriamine for ethylenediamine as the solvent. The reaction of Pb(OAc)₂·3H₂O with 1,4-benzenedithiol in diethylenetriamine at 130 °C yields the bright yellow solid [Pb(SC₆H₄S)(dien)]_n. Both compounds are stable in air over short periods: the reaction workups were performed without protection from air, while the isolated products were stored in a nitrogen-filled glovebox.

Crystal Structures. The powder diffraction pattern of [Hg(SC₆H₄S)(en)]_n was indexed to a *c*-centered monoclinic unit cell with lattice parameters of *a* = 13.147 Å, *b* = 7.121 Å, *c* = 11.630 Å, and β = 102.61°. Peak absences suggested space group *Cc* or *C2/c*. Initial structure solution by simulated annealing supported *C2/c*, with the Hg atom on a 2-fold axis and the center of the benzenedithiolate on an inversion center. Subsequent Rietveld refinement showed that this description is correct. In the refinement (Rietveld fit shown in Supporting Information, Figure S1), the benzenedithiolate was treated as a regular hexagon with the sulfurs constrained along the axis, with two internal degrees of freedom for the C–C and C–S bond lengths. The Hg atom and the ethylenediamine were treated as a single *z*-matrix with the N and C atoms restrained within the range of literature bond distances and angles. Crystal data is given in Table 1, along with lattice parameters calculated by DFT (see below).

Table 1. Crystal Data, Including Experimental and Calculated (DFT) Lattice Parameters for [Hg(SC₆H₄S)(en)]_n and [Pb(SC₆H₄S)(dien)]_n

formula	C ₈ H ₁₂ N ₂ HgS ₂	C ₁₀ H ₁₇ N ₃ PbS ₂		
<i>M_r</i>	400.91	450.61		
space group	<i>C2/c</i> (Hall - <i>C2yc</i>)	<i>P</i> $\bar{1}$ (Hall - <i>P1</i>)		
<i>Z</i>	4	2		
<i>D_x</i>	2.506 g cm ⁻³	2.217 g cm ⁻³		
radiation	synchrotron, λ = 0.70014 Å	synchrotron, λ = 0.69702 Å		
data range	3° to 36° (0.003°)	3° to 40° (0.01°)		
<i>R_{wp}</i>	8.364%	4.678%		
<i>R_{exp}</i>	6.385%	2.68%		
<i>R_{Bragg}</i>	2.615%	1.872%		
χ^2	1.716	3.049		
lattice parameters	experimental	DFT	experimental	DFT
<i>a</i>	13.1472(4)	13.078	7.3106(3) Å	7.292
<i>b</i>	7.1208(3)	7.121	10.2825(4) Å	10.293
<i>c</i>	11.6303(4)	11.617	10.2809(4) Å	10.288
α	90	90	61.186(3) deg	61.18
β	102.606(2)	101.57	86.117(3) deg	86.28
γ	90	90	86.053(3) deg	85.84

The structure of [Hg(SC₆H₄S)(en)]_n consists of one-dimensional polymers of Hg(en) linked by SC₆H₄S units, as shown in Figure 1. The polymers run along the [101]

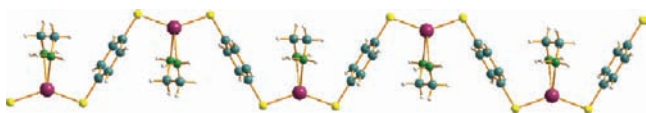


Figure 1. Structure of $[\text{Hg}(\text{SC}_6\text{H}_4\text{S})(\text{en})]_n$ determined by powder X-ray diffraction.

crystallographic direction. There are no significant interchain interactions: the shortest interchain S–S distance is 3.671(5) Å and the shortest interchain Hg–S distance is 5.088(4) Å. Within a polymer chain the Hg–S bond distance is 2.382(3) Å, slightly longer than the average of 2.34 Å for 48 reported $\text{Hg}(\text{SR})_2$ complexes.³¹

Structure solution for $[\text{Pb}(\text{SC}_6\text{H}_4\text{S})(\text{dien})]_n$ was less straightforward. The diffraction pattern was originally indexed to a *c*-centered monoclinic unit cell with lattice parameters of $a_{\text{mono}} = 17.703$ Å, $b_{\text{mono}} = 10.465$ Å, $c_{\text{mono}} = 7.310$ Å, and $\beta_{\text{mono}} = 94.55^\circ$. A structure with benzenedithiol on an inversion center and Pb on a 2-fold axis in space group *C2/c* gives a fair approximation to the measured diffraction pattern. However, in this case, the Pb atom coordinated by diethylenetriamine cannot be accommodated on a 2-fold axis. This implies either a partially disordered dien molecule in *C2/c*, or a solution in *Cc* with every atom on a general position, that is, no crystallographic symmetries aligned with molecular point symmetries. The *Cc* solution ($Z = 4$ formula units in the unit cell, $Z' = 1$ in the irreducible volume) had slightly better refined profile R_{wp} factor, but refinements of the dien group were not stable. Furthermore, there were conspicuous problems visible in the comparison of calculated and experimental data, as can be seen in Figure 2 (top).

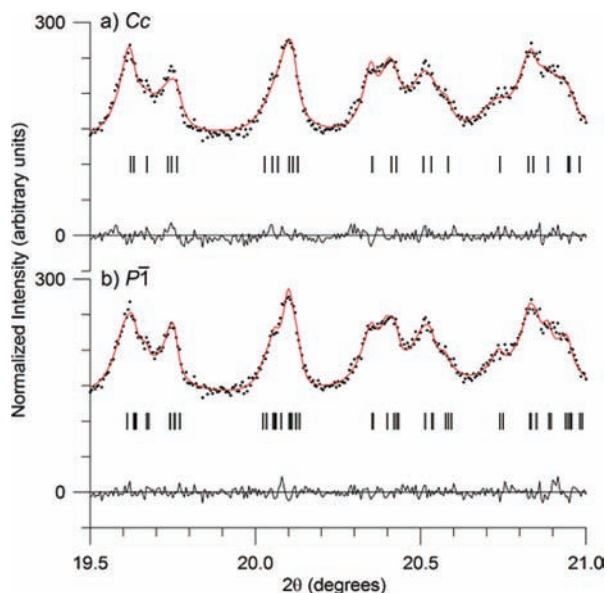


Figure 2. Comparison of a limited region of Rietveld fits for $[\text{Pb}(\text{SC}_6\text{H}_4\text{S})(\text{dien})]_n$ in the *Cc* space group (top) and *P1* space group (bottom). Experimental (black dots) versus calculated (red line) diffracted intensity, also showing peak markers and difference plots.

The observation of a number of features where the computed peak positions did not exactly match the observed values led us to suspect a small distortion to a lower, triclinic symmetry. Indeed, it was found that a solution in a triclinic cell of half the volume ($Z = 2$, $Z' = 1$) gave a slightly improved fit: $R_{\text{wp}} = 4.678\%$

vs 5.037%, with the same number of refined atomic coordinates. There is no “smoking gun” proving that the triclinic model is correct, but we regard the improvement in quality of fit as compelling. The triclinic lattice parameters listed in Table 1 span a close approximation to the original monoclinic lattice ($a' = b + c$, $b' = b - c$, $c' = a \rightarrow a' = 17.701$ Å, $b' = 10.465$ Å, $c' = 7.311$ Å, $\alpha' = 89.94^\circ$, $\beta' = 94.55^\circ$, $\gamma' = 90.01^\circ$).

Powder diffraction data has limited ability to resolve the exact configuration of the dien moiety wrapped around the Pb atom, and indeed even restrained refinements had unacceptably close contacts between adjacent molecules. Accordingly, the Pb-diethylenetriamine configuration determined by DFT calculations (see below) was used as a rigid body in the refinement (Rietveld fit shown in Supporting Information, Figure S2).

The structure of $[\text{Pb}(\text{SC}_6\text{H}_4\text{S})(\text{dien})]_n$ is more complex than that of $[\text{Hg}(\text{SC}_6\text{H}_4\text{S})(\text{en})]_n$. The coordination sphere of Pb in $[\text{Pb}(\text{SC}_6\text{H}_4\text{S})(\text{dien})]_n$ is shown in Figure 3. Each Pb atom is

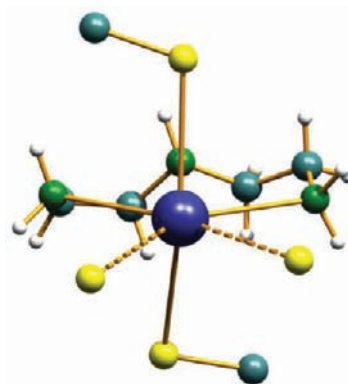


Figure 3. Coordination sphere of Pb in $[\text{Pb}(\text{SC}_6\text{H}_4\text{S})(\text{dien})]_n$.

coordinated by the three N atoms of a dien molecule. There are four sulfur atoms within a distance of Pb that indicates some interaction, with Pb–S distances of 2.96(1), 3.07(2), 3.27(1), and 3.65(2) Å. If the two shorter Pb–S interactions at 2.96 and 3.07 Å are considered to be regular covalent bonds (shown as solid lines in Figure 3) and the two longer Pb–S interactions at 3.27 and 3.65 Å are considered to be Pb←S dative bonds (shown as dashed lines in Figure 3), then a bonding scheme that includes only the Pb–S regular covalent bonds yields the one-dimensional polymer shown in Figure 4. Those chains run

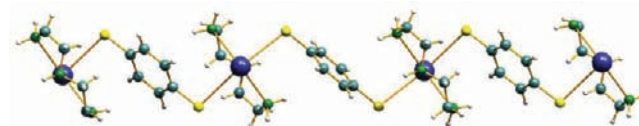


Figure 4. One-dimensional chains in $[\text{Pb}(\text{SC}_6\text{H}_4\text{S})(\text{dien})]_n$.

along the $[-111]$ crystallographic direction. If both the short and the long Pb–S interactions are considered, then chains of corner-sharing Pb_2S_2 parallelograms are also present, as shown in Figure 5. In Figure 5 the 4-sulfur coordination sphere of each Pb is evident, with the two dative Pb–S bonds oriented “forward” and “backward” on alternating Pb atoms. The corner-sharing Pb_2S_2 parallelogram chains run along the $[100]$ crystallographic direction.

Spectroscopy, Band Gap, and Conductivity. Figure 6 shows the diffuse reflectance UV–visible spectrum of $[\text{Hg}(\text{SC}_6\text{H}_4\text{S})(\text{en})]_n$ and Figure 7 shows the diffuse reflectance

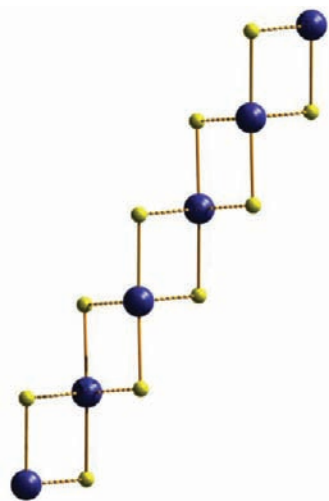


Figure 5. Corner-sharing Pb_2S_2 parallelograms in $[\text{Pb}(\text{SC}_6\text{H}_4\text{S})(\text{dien})]_n$ with short Pb–S interactions shown as solid bonds and long (dative) Pb–S interactions shown as dashed bonds.

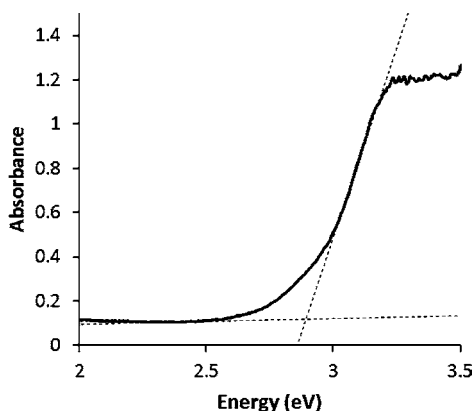


Figure 6. Diffuse reflectance UV–visible spectrum of $[\text{Hg}(\text{SC}_6\text{H}_4\text{S})(\text{en})]_n$.

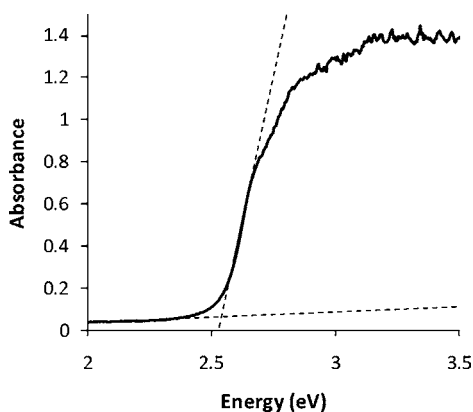


Figure 7. Diffuse reflectance UV–visible spectrum of $[\text{Pb}(\text{SC}_6\text{H}_4\text{S})(\text{dien})]_n$.

UV–visible spectrum of $[\text{Pb}(\text{SC}_6\text{H}_4\text{S})(\text{dien})]_n$. Extrapolation of the absorbance edge to the baseline indicates a band gap of 2.89 eV for $[\text{Hg}(\text{SC}_6\text{H}_4\text{S})(\text{en})]_n$ and 2.54 eV for $[\text{Pb}(\text{SC}_6\text{H}_4\text{S})(\text{dien})]_n$. The absorption onset for $[\text{Hg}(\text{SC}_6\text{H}_4\text{S})(\text{en})]_n$ is more gradual than that of $[\text{Pb}(\text{SC}_6\text{H}_4\text{S})(\text{dien})]_n$, which makes the

determination of the band gap from the spectrum of $[\text{Hg}(\text{SC}_6\text{H}_4\text{S})(\text{en})]_n$ somewhat uncertain, and its band gap may be somewhat less than 2.89 eV.

Because of the relatively large band gaps for the two compounds, any electrical conductivity of the undoped materials was expected to be small. Simple two-point measurements of pressed powders of $[\text{Pb}(\text{SC}_6\text{H}_4\text{S})(\text{dien})]_n$ and $[\text{Hg}(\text{SC}_6\text{H}_4\text{S})(\text{en})]_n$ were performed. The conductivity of both compounds is less than $1 \times 10^{-12} \Omega^{-1}\text{cm}^{-1}$, the limit of detection of our experimental setup.

Electronic Structure Calculations and Their Relationship to the Structure and Properties of $[\text{Hg}(\text{SC}_6\text{H}_4\text{S})(\text{en})]_n$ and $[\text{Pb}(\text{SC}_6\text{H}_4\text{S})(\text{dien})]_n$. The relatively simple one-dimensional structures of $[\text{Hg}(\text{SC}_6\text{H}_4\text{S})(\text{en})]_n$ and $[\text{Pb}(\text{SC}_6\text{H}_4\text{S})(\text{dien})]_n$ make them good materials in which to examine correlations between structure/composition and electronic structure. We therefore performed DFT band structure calculations on both $[\text{Hg}(\text{SC}_6\text{H}_4\text{S})(\text{en})]_n$ and $[\text{Pb}(\text{SC}_6\text{H}_4\text{S})(\text{dien})]_n$.

The crystallographically determined structures of $[\text{Hg}(\text{SC}_6\text{H}_4\text{S})(\text{en})]_n$ and $[\text{Pb}(\text{SC}_6\text{H}_4\text{S})(\text{dien})]_n$ were used as starting points for a structure optimization in the DFT calculations. The crystallographic space group of each was maintained, while the lattice parameters (and, of course, atomic positions) were allowed to optimize. In both cases the calculated structures were very similar to the crystallographic ones. In Table 1 the crystallographic and calculated lattice parameters of both compounds can be compared. Table 2 gives

Table 2. Crystallographic and Calculated Bond Distances [Å] for $[\text{Hg}(\text{SC}_6\text{H}_4\text{S})(\text{en})]_n$ and $[\text{Pb}(\text{SC}_6\text{H}_4\text{S})(\text{dien})]_n$

	experimental	calculated
Hg–S	2.382(3)	2.432
Hg–N	2.566(9)	2.496
Pb–S1 (axial)	2.96(1)	2.876
Pb–S1b (axial)	3.07(2)	3.095
Pb–S1 (equatorial)	3.27(1)	3.334
Pb–S1b (equatorial)	3.65(2)	3.402

the selected bond distances from the crystal structure and calculations for both $[\text{Hg}(\text{SC}_6\text{H}_4\text{S})(\text{en})]_n$ and $[\text{Pb}(\text{SC}_6\text{H}_4\text{S})(\text{dien})]_n$.

The calculated electronic band structure and density of states for $[\text{Pb}(\text{SC}_6\text{H}_4\text{S})(\text{dien})]_n$ and $[\text{Hg}(\text{SC}_6\text{H}_4\text{S})(\text{en})]_n$ are plotted in Figures 8 and 9, respectively. The band gap calculated for $[\text{Hg}(\text{SC}_6\text{H}_4\text{S})(\text{en})]_n$ is 2.24 eV and for $[\text{Pb}(\text{SC}_6\text{H}_4\text{S})(\text{dien})]_n$ is 2.10 eV. The calculated values are 0.65 and 0.44 eV smaller, respectively, than those determined by diffuse reflectance spectroscopy; DFT-calculated band gaps are typically lower than the experimental values.³² Additionally, as mentioned above, the band gap of $[\text{Hg}(\text{SC}_6\text{H}_4\text{S})(\text{en})]_n$ may in fact be somewhat lower than the 2.89 eV determined by diffuse reflectance spectroscopy.

In $[\text{Pb}(\text{SC}_6\text{H}_4\text{S})(\text{dien})]_n$ sulfur states, and, to a lesser extent, carbon states, make the major contribution to the top of the valence band and carbon states dominate the bottom of the conduction band, as can be seen in Figure 8. In Figure 10 the electron density associated with the highest occupied and lowest unoccupied states (at the *T* point of the Brillouin zone; points in the Brillouin zone are defined here³³) of $[\text{Pb}(\text{SC}_6\text{H}_4\text{S})(\text{dien})]_n$ are shown. The electron density around the $\text{SC}_6\text{H}_4\text{S}$ fragment at the valence band edge bears a striking

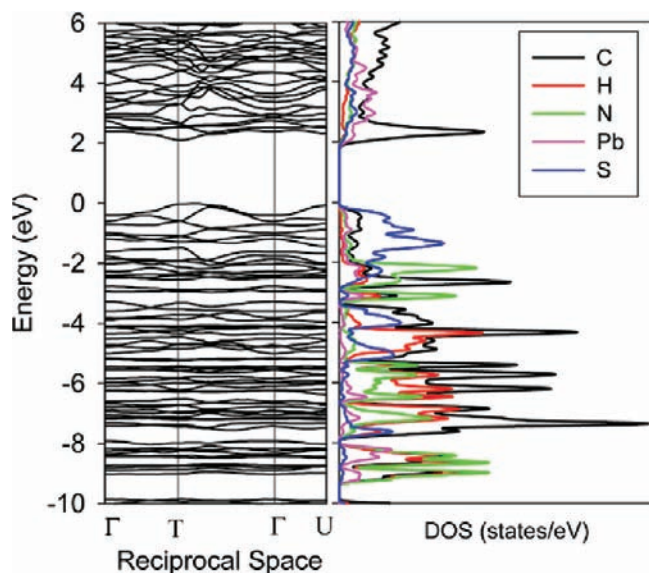


Figure 8. Calculated electronic band structure and density of states of $[\text{Pb}(\text{SC}_6\text{H}_4\text{S})(\text{dien})]_n$. The highest occupied state is set to 0 eV.

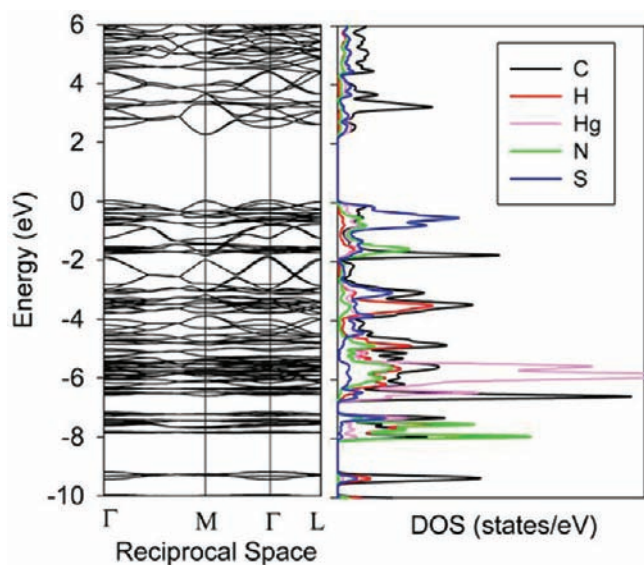


Figure 9. Calculated electronic band structure and density of states of $[\text{Hg}(\text{SC}_6\text{H}_4\text{S})(\text{en})]_n$. The highest occupied state is set to 0 eV.

resemblance to the HOMO of an isolated $\text{SC}_6\text{H}_4\text{S}^-$ dianion, as determined by a simple Hückel calculation (see Figure 12). Similarly, the electron density around the $\text{SC}_6\text{H}_4\text{S}$ fragment at the conduction band edge resembles the LUMO of an isolated $\text{SC}_6\text{H}_4\text{S}^-$ dianion, as shown in Figure 12. Thus it appears that the electronic structure of $[\text{Pb}(\text{SC}_6\text{H}_4\text{S})(\text{dien})]_n$ can be fairly well described as the sum of the ionic components $\text{Pb}(\text{dien})^{2+}$ and $\text{SC}_6\text{H}_4\text{S}^-$, with the $\text{SC}_6\text{H}_4\text{S}^-$ HOMO and LUMO states dominant at the band edges. The Pb states in the calculated band structure are also consistent with the presence of Pb^{2+} : there are filled Pb 6s states near the bottom of the upper valence band (at about -8 eV) and Pb 6p states in the conduction band.³⁴ Because the states at both the valence and the conduction band edges are mainly due to $\text{SC}_6\text{H}_4\text{S}^-$ units, which do not interact significantly with each other, the band dispersions in $[\text{Pb}(\text{SC}_6\text{H}_4\text{S})(\text{dien})]_n$ are quite narrow; the

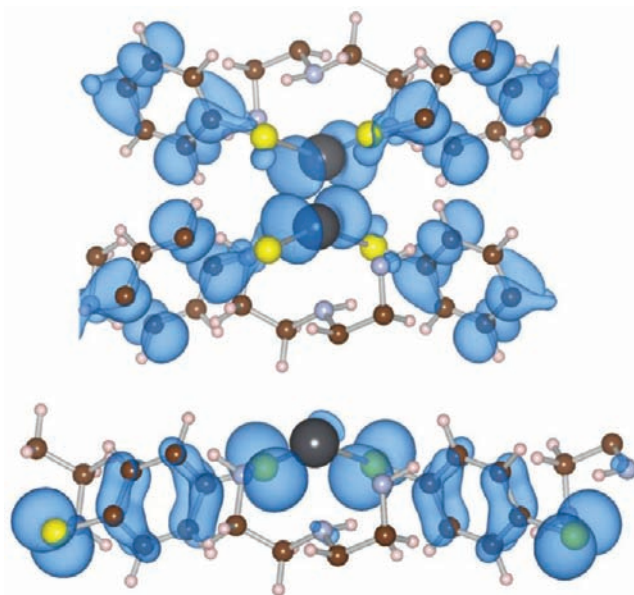


Figure 10. Calculated electron density (square of the electronic wave function) associated with the highest occupied (bottom) and lowest unoccupied (top) states at the T point of the Brillouin zone for $[\text{Pb}(\text{SC}_6\text{H}_4\text{S})(\text{dien})]_n$.

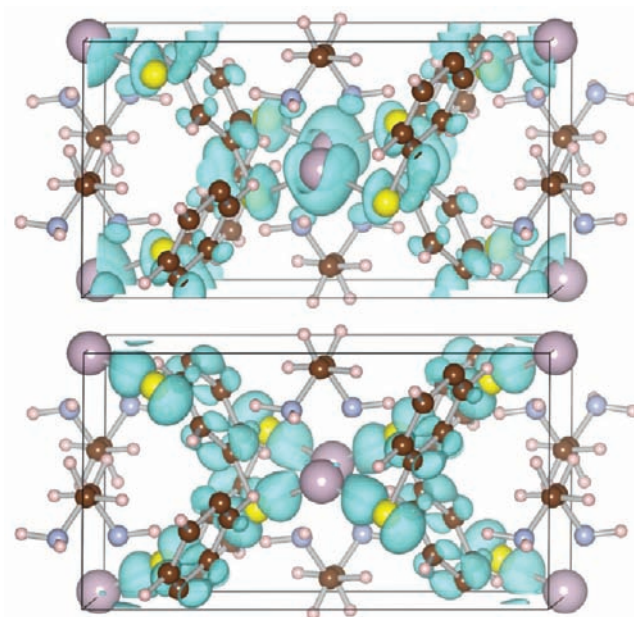


Figure 11. Calculated electron density (square of the electronic wave function) associated with the highest occupied (bottom) and lowest unoccupied (top) states at the M point of the Brillouin zone for $[\text{Hg}(\text{SC}_6\text{H}_4\text{S})(\text{en})]_n$.

bands at the T point are too flat to extract a meaningful electron or hole effective mass.

In some hybrid inorganic–organic materials that contain a semiconducting component, the electron or hole movement occurs only through the inorganic component, while the organic component is a passive insulator. The prime example of such materials are the $\text{ME}(\text{da})_{0.5}$ ($M = \text{Cd}, \text{Zn}$; $E = \text{S}, \text{Se}, \text{Te}$; $\text{da} =$ diamine such as ethylenediamine) layered compounds.^{35–39} In $[\text{Pb}(\text{SC}_6\text{H}_4\text{S})(\text{dien})]_n$ there are purely inorganic corner-sharing Pb_2S_2 parallelogram chains, as shown

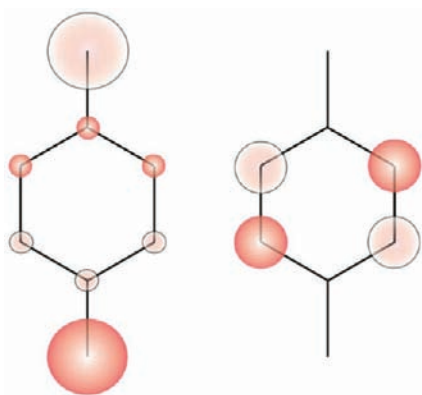


Figure 12. HOMO (left) and LUMO (right) of the $^{-}\text{SC}_6\text{H}_4\text{S}^{-}$ dianion, calculated by the Hückel method.

in Figure 5. Those chains run along the $[-111]$ direction. An examination of the bands at the R point, which corresponds to the $[-111]$ direction, shows no significant band dispersion, nor a larger contribution from Pb at the band edges. Thus it seems that extended polymers of an inorganic component within a hybrid material do not necessarily lead to semiconductivity through those inorganic polymers. That conclusion is consistent with observations by us and others in systems that contain purely inorganic networks (if dative bonds are included). For example, the compound $[\text{Pb}_3(\text{SC}_6\text{H}_4\text{S})_3(\text{en})_2]_n$ contains Pb–S infinite two-dimensional networks,¹⁰ while $[\text{Tl}_2(\text{SC}_6\text{H}_4\text{S})]_n$ and $[\text{Tl}_2(\text{SeC}_6\text{H}_4\text{Se})]_n$ contain Tl–S and Tl–Se infinite two-dimensional networks,⁴⁰ yet none of these compounds has significant electrical conductivity at room temperature. The simple metal thiolates $\text{Cd}(\text{SPh})_2$,⁴¹ $\text{Pb}(\text{SPh})_2$,⁴² $\text{Pb}(\text{SCH}_2\text{CH}_2\text{S})$,⁴³ and AgSR ⁴⁴ ($R = n$ -alkyl or aryl) all contain infinite M–S networks, yet none are reported to be semiconducting. Similarly, cadmium thiolate clusters linked by RS^- ($R = \text{aryl}$) anions to form infinite networks are known,^{45,46} but no electrical conductivity has been reported for any of those materials.

In $[\text{Hg}(\text{SC}_6\text{H}_4\text{S})(\text{en})]_n$ the main atomic contributions to the top of the valence band are from sulfur and carbon (see Figure 9), as in $[\text{Pb}(\text{SC}_6\text{H}_4\text{S})(\text{dien})]_n$. The electron density associated with the highest occupied state (at the M point) is shown in Figure 11, and the electron density around the $\text{SC}_6\text{H}_4\text{S}$ resembles the Hückel-calculated HOMO of the $^{-}\text{SC}_6\text{H}_4\text{S}^{-}$ dianion, just as in $[\text{Pb}(\text{SC}_6\text{H}_4\text{S})(\text{dien})]_n$. In contrast, the states near the conduction band edge (at M) are quite different from those in $[\text{Pb}(\text{SC}_6\text{H}_4\text{S})(\text{dien})]_n$. In Figure 9 the states at the band edge include significant contributions from carbon, sulfur, and mercury, in stark contrast to $[\text{Pb}(\text{SC}_6\text{H}_4\text{S})(\text{dien})]_n$ where carbon dominates the states at the conduction band edge (see Figure 8). The (empty) electron density on mercury at the conduction band edge at the M point is visible in Figure 11, right panel. The electron density consists, essentially, of the Hg 6s orbital, which is empty in Hg^{2+} , perturbed to the side of the atom opposite the en ligand.

The presence of the empty Hg 6s atomic orbital leads to hybridization between the metal and organic components in $[\text{Hg}(\text{SC}_6\text{H}_4\text{S})(\text{en})]_n$, and thereby some moderate band dispersion in its conduction band, especially around the M point. The M point of the Brillouin zone corresponds to the polymer chain orientation in real space. Fitting the conduction band dispersion around the M point yields an averaged electron effective mass of $0.29 \cdot m_e$, which falls into the range of typical

semiconductors, and indicates that electron conduction may be feasible in this class of materials. For comparison, the isotropic electron effective mass in HgS is $0.10 \cdot m_e$.⁴⁷ Any free electrons in $[\text{Hg}(\text{SC}_6\text{H}_4\text{S})(\text{en})]_n$ will therefore have fairly good mobility along the polymer chains, and the low conductivity of $[\text{Hg}(\text{SC}_6\text{H}_4\text{S})(\text{en})]_n$ is due to the very low carrier concentration in this wide-bandgap, undoped semiconductor.

CONCLUSIONS

In $[\text{Pb}(\text{SC}_6\text{H}_4\text{S})(\text{dien})]_n$ the electronic states at the band edges are essentially the HOMO and LUMO of the $^{-}\text{SC}_6\text{H}_4\text{S}^{-}$ dianion, so the band gap of $[\text{Pb}(\text{SC}_6\text{H}_4\text{S})(\text{dien})]_n$ is largely determined by the HOMO–LUMO gap of the $\text{SC}_6\text{H}_4\text{S}$ organosulfur fragment. In contrast, in $[\text{Hg}(\text{SC}_6\text{H}_4\text{S})(\text{en})]_n$ the empty Hg 6s orbital is a major component of the conduction band edge. The Hg 6s orbital hybridizes with the $\text{SC}_6\text{H}_4\text{S}$ fragment in the conduction band, leading to moderate band dispersion and, theoretically, reasonable electron mobility along the polymer chains. However, the hybridization of the Hg 6s orbital with the $\text{SC}_6\text{H}_4\text{S}$ fragment leads to a somewhat larger band gap for $[\text{Hg}(\text{SC}_6\text{H}_4\text{S})(\text{en})]_n$. Hybrid materials with higher conductivity are likely to be obtained with organic components with smaller HOMO–LUMO gaps, generally leading to smaller band gaps in the hybrid materials. The selection of metal will also be critical, and should be chosen such that unoccupied metal orbitals will have energies near the conduction band edge and/or occupied metal orbitals will have energies near the valence band edge.

ASSOCIATED CONTENT

Supporting Information

Rietveld refinement plots for $[\text{Hg}(\text{SC}_6\text{H}_4\text{S})(\text{en})]_n$ and $[\text{Pb}(\text{SC}_6\text{H}_4\text{S})(\text{dien})]_n$, DFT-calculated structures for $[\text{Hg}(\text{SC}_6\text{H}_4\text{S})(\text{en})]_n$ and $[\text{Pb}(\text{SC}_6\text{H}_4\text{S})(\text{dien})]_n$ as text (in CIF format) in the SI PDF, and CIFs for the structures of $[\text{Hg}(\text{SC}_6\text{H}_4\text{S})(\text{en})]_n$ and $[\text{Pb}(\text{SC}_6\text{H}_4\text{S})(\text{dien})]_n$ determined by X-ray diffraction. This material is available free of charge via the Internet at <http://pubs.acs.org>.

AUTHOR INFORMATION

Corresponding Author

*E-mail: tpvaid@ua.edu.

Present Addresses

[†]Novus International, 20 Research Park Drive, St. Charles, MO 63304.

[‡]Materials Sciences Division, Lawrence Berkeley Lab, Berkeley, CA 94720.

ACKNOWLEDGMENTS

This work was supported by the University of Alabama. Computations were performed on the University of Bath's High Performance Computing Facility, and facilitated by membership of the UK's HPC Materials Chemistry Consortium, which is funded by EPSRC (Grant No. EP/F067496). Use of the National Synchrotron Light Source, Brookhaven National Laboratory, was supported by the U.S. Department of Energy, Office of Basic Energy Sciences, under Contract No. DE-AC02-98CH10886.

REFERENCES

- Yaghi, O. M.; O'Keeffe, M.; Ockwig, N. W.; Chae, H. K.; Eddaoudi, M.; Kim, J. *Nature* **2003**, *423*, 705–714.

- (2) O'Keeffe, M.; Peskov, M. A.; Ramsden, S. J.; Yaghi, O. M. *Acc. Chem. Res.* **2008**, *41*, 1782–1789.
- (3) Natarajan, S.; Mahata, P. *Chem. Soc. Rev.* **2009**, *38*, 2304–2318.
- (4) Farha, O. K.; Hupp, J. T. *Acc. Chem. Res.* **2010**, *43*, 1166–1175.
- (5) Meek, S. T.; Greathouse, J. A.; Allendorf, M. D. *Adv. Mater.* **2011**, *23*, 249–267.
- (6) Wong-Foy, A. G.; Matzger, A. J.; Yaghi, O. M. *J. Am. Chem. Soc.* **2006**, *128*, 3494–3495.
- (7) Bae, T.-H.; Lee, J. S.; Qiu, W.; Koros, W. J.; Jones, C. W.; Nair, S. *Angew. Chem., Int. Ed.* **2010**, *49*, 9863–9866.
- (8) Kreno, L. E.; Hupp, J. T.; Van Duyne, R. P. *Anal. Chem.* **2010**, *82*, 8042–8046.
- (9) Cheetham, A. K.; Rao, C. N. R. *Science* **2007**, *318*, 58–59.
- (10) Turner, D. L.; Vaid, T. P.; Stephens, P. W.; Stone, K. H.; DiPasquale, A. G.; Rheingold, A. L. *J. Am. Chem. Soc.* **2008**, *130*, 14–15.
- (11) Turner, D. L.; Stone, K. H.; Stephens, P. W.; Vaid, T. P. *Dalton Trans.* **2010**, *39*, 5070–5073.
- (12) Reed, M. A.; Zhou, C.; Muller, C. J.; Burgin, T. P.; Tour, J. M. *Science* **1997**, *278*, 252–254.
- (13) Nitzan, A.; Ratner, M. A. *Science* **2003**, *300*, 1384–1389.
- (14) Yeganeh, S.; Ratner, M. A.; Galperin, M.; Nitzan, A. *Nano Lett.* **2009**, *9*, 1770–1774.
- (15) Tsuji, Y.; Staykov, A.; Yoshizawa, K. *J. Am. Chem. Soc.* **2011**, *133*, 5955–5965.
- (16) Boardman, B. M.; Widawsky, J. R.; Park, Y. S.; Schenck, C. L.; Venkataraman, L.; Steigerwald, M. L.; Nuckolls, C. *J. Am. Chem. Soc.* **2011**, *133*, 8455–8457.
- (17) Testaferri, L.; Tiecco, M.; Tingoli, M.; Chianelli, D.; Montanucci, M. *Synthesis* **1983**, 751–755.
- (18) Adams, R.; Ferretti, A. *J. Am. Chem. Soc.* **1959**, *81*, 4939–4940.
- (19) Porter, W. W.; Vaid, T. P. *J. Org. Chem.* **2005**, *70*, 5028–5035.
- (20) Coelho, A. A. *J. Appl. Crystallogr.* **2003**, *36*, 86–95.
- (21) Hohenberg, P.; Kohn, W. *Phys. Rev.* **1964**, *136*, B864.
- (22) Kohn, W.; Sham, L. J. *Phys. Rev.* **1965**, *140*, A1133.
- (23) Perdew, J. P.; Ruzsinszky, A.; Csonka, G. I.; Vydrov, O. A.; Scuseria, G. E.; Constantin, L. A.; Zhou, X.; Burke, K. *Phys. Rev. Lett.* **2008**, *100*, 136406.
- (24) Havu, V.; Blum, V.; Havu, P.; Scheffler, M. *J. Comput. Phys.* **2009**, *228*, 8367–8379.
- (25) Blum, V.; Gehrke, R.; Hanke, F.; Havu, P.; Havu, V.; Ren, X.; Reuter, K.; Scheffler, M. *Comput. Phys. Commun.* **2009**, *180*, 2175–2196.
- (26) Payne, M. C.; Teter, M. P.; Allan, D. C.; Arias, T. A.; Joannopoulos, J. D. *Rev. Mod. Phys.* **1992**, *64*, 1045–1097.
- (27) Vanlenthe, E.; Baerends, E. J.; Snijders, J. G. *J. Chem. Phys.* **1994**, *101*, 9783–9792.
- (28) Glans, P. A.; Learmonth, T.; McGuinness, C.; Smith, K. E.; Guo, J. H.; Walsh, A.; Watson, G. W.; Egdell, R. G. *Chem. Phys. Lett.* **2004**, *399*, 98–101.
- (29) Glans, P. A.; Learmonth, T.; Smith, K. E.; Guo, J.; Walsh, A.; Watson, G. W.; Terzi, F.; Egdell, R. G. *Phys. Rev. B* **2005**, *71*, 235109.
- (30) Schrauzer, G. N.; Prakash, H. *Inorg. Chem.* **1975**, *14*, 1200–1204.
- (31) Manceau, A.; Nagy, K. L. *Dalton Trans.* **2008**, 1421–1425.
- (32) Godby, R. W.; Schlüter, M.; Sham, L. J. *Phys. Rev. B* **1988**, *37*, 10159–10175.
- (33) Bilbao Crystallographic Server. <http://www.cryst.ehu.es/>.
- (34) Walsh, A.; Payne, D. J.; Egdell, R. G.; Watson, G. W. *Chem. Soc. Rev.* **2011**, *40*, 4455–4463.
- (35) Huang, X.; Li, J.; Fu, H. *J. Am. Chem. Soc.* **2000**, *122*, 8789–8790.
- (36) Huang, X.; Heulings, H. R. I. V.; Le, V.; Li, J. *Chem. Mater.* **2001**, *13*, 3754–3759.
- (37) Heulings, H. R. I. V.; Huang, X.; Li, J.; Yuen, T.; Lin, C. L. *Nano Lett.* **2001**, *1*, 521–525.
- (38) Huang, X.; Li, J.; Zhang, Y.; Mascarenhas, A. *J. Am. Chem. Soc.* **2003**, *125*, 7049–7055.
- (39) Fu, H.; Li, J. *J. Chem. Phys.* **2004**, *120*, 6721–6725.
- (40) Stone, K. H.; Turner, D. L.; Singh, M. P.; Vaid, T. P.; Stephens, P. W. *Acta Crystallogr., Sect. B* **2011**, *67*, 409–415.
- (41) Dance, I. G.; Garbutt, R. G.; Craig, D. C.; Scudder, M. L. *Inorg. Chem.* **1987**, *26*, 4057–4064.
- (42) Rae, A. D.; Craig, D. C.; Dance, I. G.; Scudder, M. L.; Dean, P. A. W.; Kmetc, M. A.; Payne, N. C.; Vittal, J. J. *Acta Crystallogr., Sect. B* **1997**, *53*, 457–465.
- (43) Dean, P. A. W.; Vittal, J. J.; Payne, N. C. *Inorg. Chem.* **1985**, *24*, 3594–3597.
- (44) Dance, I. G.; Fisher, K. J.; Banda, R. M. H.; Scudder, M. L. *Inorg. Chem.* **1991**, *30*, 183–187.
- (45) Dance, I. G.; Garbutt, R. G.; Scudder, M. L. *Inorg. Chem.* **1990**, *29*, 1571–1575.
- (46) Zhang, Q.; Lin, Z.; Bu, X.; Wu, T.; Feng, P. *Chem. Mater.* **2008**, *20*, 3239–3241.
- (47) Madelung, O. *Semiconductors: Data Handbook*, 3rd ed.; Springer: New York, 2004.